

APPLICATION OF SEMI-EMPIRICAL MODELS OF ELECTRON BEAM CONTROL IN RADIATION STERILIZATION TECHNOLOGY

Valentín T. Lazurik^{1*}, Igor O. Girka¹, Oleksandr O. Zolotukhin¹, Zbigniew Zimek²

¹V.N. Karazin Kharkiv National University, Kharkiv, Ukraine

²Institute of Nuclear Chemistry and Technology, Warsaw, Poland

*Corresponding Author e-mail: vtlazurik@karazin.ua

Received February 3, 2026; revised March 30, 2026; accepted April 22, 2026

An application of semi-empirical models involves analyzing data regularly recorded during irradiation control and processing it to determine the values of the semi-empirical model parameters. In the present paper, the recorded data used present the depth dose curves measured at the INCT radiation sterilization center in Warsaw, Poland. The measurement method is described. The depth dose curves are analyzed using the dosimetric wedge method. The characteristics of the depth dose curves are presented. The depth ranges are determined within which the measurement results can be used without special processing as depth dose curve values in the dosimetric wedge. Special procedures are developed to approximate and extrapolate the measurement results. The objective of the procedures is to obtain the basic dependencies of semi-empirical models, namely the doses as a function of depth at normal incidence of the electron beam on a semi-infinite medium. Special procedures are developed to process measurement results using the PFSEM method (two-parameter fitting of a semi-empirical model of depth-dose curves). A procedure for excluding bremsstrahlung contributions from depth-dose curves is proposed and implemented. The value of this contribution is estimated as the average dose in the bremsstrahlung tail region. The change of the bremsstrahlung influence on the doses with depth is neglected. The method for selecting the values of model-fitting parameters is proposed based on the assumption that the fitting parameters depend weakly on electron energy. Based on the proposed method, the fitting parameters of semi-empirical models are determined from Monte Carlo simulations of depth-dose curves during irradiation of a layer with a monoenergetic electron beam. The measurement results are compared with depth-dose curves calculated using semi-empirical models for electron-beam irradiation at different angles of incidence on an aluminum dosimetric wedge. Based on the comparison results, the errors in model predictions and the feasibility of implementing methods to optimize irradiation processes by selecting the angle of electron incidence on the surface of the irradiated object are discussed.

Keywords: Electron beam dosimetry; Depth Dose curve; Sterilization; Control of optimal modes; Semi-empirical model; Monte-Carlo method

PACS: 87.53.Bn, 02.60.Cb

INTRODUCTION

Radiation technologies are widely used to sterilize pharmaceutical products and medical equipment and to disinfect food products. Optimizing irradiation is one of the main tasks in implementing radiation technologies [1-16]. In radiation technologies, the minimum level of dose uniformity (*DUR*) in the irradiated object corresponds to the optimal irradiation mode [17-25]. For electron beams, the two-sided irradiation method is the one that enables low *DUR* [4,5]. When using this method, the optimal irradiation mode of the layer is achieved when, at a given electron energy E , the layer has an optimal thickness $H_{opt}(E)$. At the same time, there is a strong dependence of *DUR* on layer thickness, which poses technical challenges to implementing the optimal mode of two-sided irradiation at fixed electron energy. Changing the angle of incidence of the electron beam on the surface of the irradiated object is one possible solution to the technical problems encountered in implementing the two-sided irradiation method [26-34]. The feasibility of this approach for optimizing irradiation was demonstrated by reviewing the results of Monte Carlo modeling of depth-dose curves [26]. It should be noted that the capabilities of such modeling of the depth dose distribution for given angles of incidence of the electron beam on the layer were implemented in the *RT-Office* software (*ModeRTL* module). However, these capabilities were not used to optimize the irradiation in radiation technologies, since such a knowledge-intensive optimization procedure is difficult to implement in technology centers.

Therefore, new tasks arose in electron radiation dosimetry related to the need to investigate the dependence of the depth dose distribution on the angle of incidence of the electron beam on the material layer. To carry out these studies, semi-empirical models of the depth dose curve caused by an electron beam incident on the surface of a layer at an angle θ were developed. In these semi-empirical models [27,28], the distribution of transferred energy in the volume of matter, which is initiated when a point beam of radiation strikes the surface of a semi-infinite medium at a normal angle, is the basic object (*Dose-Map* object). The following assumptions were used to develop the models. The *Dose-Map* object was assumed to have axial symmetry with respect to the beam particles' direction of incidence on the layer. The parameters of the object in its eigen coordinate system were assumed to be independent on the angle of incidence of the beam on the layer of substance. Finally, the dose distribution was assumed to be uniform or normal (Gaussian) across the object's cross-sections at all depths within the layer. Based on these assumptions, two two-parameter semi-

empirical models were developed: *SEM2U* – a model with uniform dose distribution, and *SEM2N* – a model with normal dose distribution in the cross-sections of the *Dose-Map* object.

A comparison of the depth dose curves obtained using the developed semi-empirical models *SEM2U* and *SEM2N* with the depth dose curves obtained by Monte Carlo simulation at different angles θ of the electron beam incidence on the layer demonstrated satisfactory agreement of these results for cases of monoenergetic electron beams at incidence angles $0^\circ < \theta < 60^\circ$ on a semi-infinite layer. In [27], examples were given where the developed two-parameter models provided the correct calculation of two technological characteristics of the double-sided irradiation simultaneously (in a coordinated manner): the optimal target thickness and the dose uniformity ratio in the target.

To implement methods for optimizing irradiation based on selecting the angle of incidence of electrons on the surface of the irradiated object, the semi-empirical models and the software developed on the basis of these models can be used. However, for the practical implementation of these developments, the proposed optimization methods should be approved and the software should be verified. In the present paper, the semi-empirical models are validated by the results of dose depth distribution curve measurements carried out at the INCT radiation sterilization centre in Warsaw, Poland.

The data recorded during the control of irradiation at this radiation sterilization centre is analyzed. The measurement method used is described. The characteristics of the depth dose curve measurements carried out by the dosimetric wedge method are analyzed. The depth ranges within which the measurement results can be used without special processing as depth dose curve values in the dosimetric wedge are determined. Special procedures for approximation and extrapolation of measurement results are used to obtain the values of the basic model: the values of the doses subject to the depth at normal incidence of the electron beam on a semi-infinite medium. Special procedures for processing measurement results are developed based on the *PFSEM* method (fitting of semi-empirical model parameters) [8]. The special procedure is used to exclude the contribution of bremsstrahlung to the depth dose curves. The procedure is based on the estimate of this contribution as the average dose value in the bremsstrahlung tail region.

The methods for determining the fitting parameters of semi-empirical models are analyzed. The method is proposed for selecting the values of the model fitting parameters. The method is based on the assumption of a weak dependence of the fitting parameters on the electron energy. Based on the proposed method, the fitting parameters of semi-empirical models are determined based on the results of Monte Carlo simulation of depth dose curves during irradiation of a layer with electron beams of different energies. The possibilities of implementing various methods for determining model fitting parameters in the practical activities of radiation sterilization centers are discussed.

The measurement results are compared with the results of calculating depth dose curves using semi-empirical models, when irradiating a layer with electron beams at different angles of incidence on the layer. The errors in the model predictions are discussed and recommendations are given for the implementation of methods for optimizing irradiation processes based on the selection of the angle of incidence of electrons on the surface of the irradiated object.

METHOD FOR VALIDATION OF SEMI-EMPIRICAL MODELS IN A RADIATION STERILIZATION CENTER

Measurement of depth dose curves at specified angles of incidence of the electron beam on the surface of the irradiated object

To validate the semi-empirical models, the radiation characteristics recorded at the radiation sterilization center are determined first. This is necessary to reconcile the data on the characteristics of the irradiation process available at this centre with the parameters of the semi-empirical models, which are required to calculate these characteristics. To test the semi-empirical models, the results of measurements of depth dose distribution curves in objects exposed to radiation at the Radiation Sterilization Center of the Institute of Nuclear Chemistry and Technology in Warsaw, Poland, are used. At this centre, uniform irradiation of the surface of objects was ensured by the uniform motion of objects on a conveyor line and scanning with an electron beam in a direction perpendicular to the direction of the conveyor motion. Changes in the angle of incidence θ of the electron beam on the surface of the object were achieved by changing the spatial orientation of the irradiated object on the conveyor. For this purpose, the object was placed on a platform with a specified angle of inclination. The schematic of the method for measuring depth dose curves at specified angles of incidence of the electron beam on the surface of the irradiated object is shown in Fig. 1.

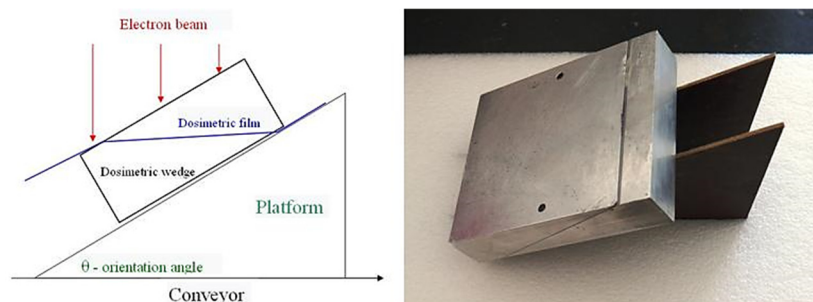


Figure 1. Schematic of measuring the depth dose curve at a given angle of incidence of the electron beam on the surface of the irradiated object

It should be noted that when using this method of measuring depth dose curves, it is necessary to take into account the change in the electron flux $\Phi(\theta)$ incident on the surface of the object when the angle θ of the irradiated object changes $\Phi(\theta) = \Phi_0 \cos(\theta)$.

The depth dose curves were measured using an aluminum dosimetric wedge from GEX Corporation, which characteristics are presented in Fig. 2.

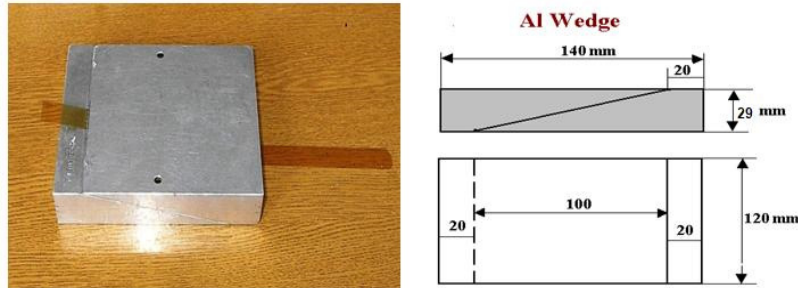


Figure 2. Aluminum dosimetric wedge for measuring depth dose curves

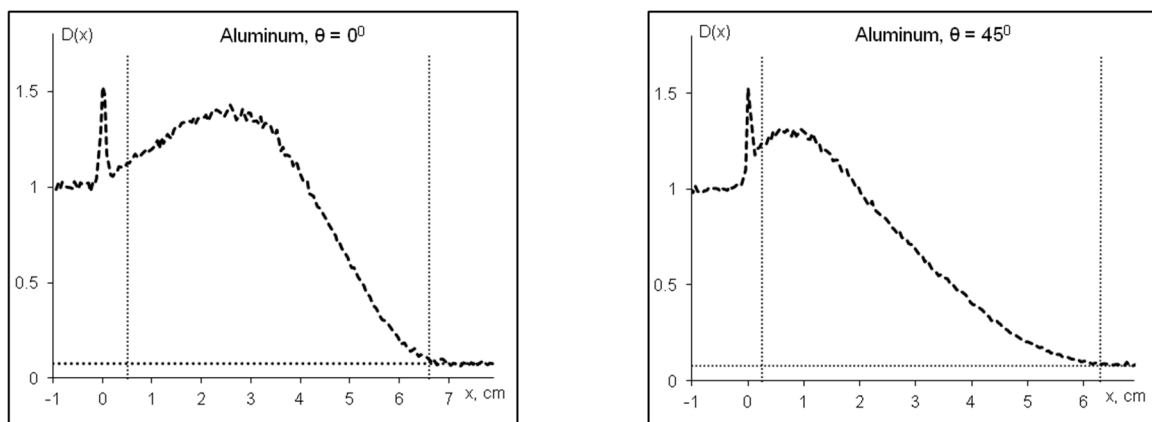


Figure 3. Results of measurements of depth dose curves in dosimetric film obtained by the dosimetric wedge method

The dose values D_i , determined at a set of points on the dosimetric film, are the measurement results. The starting point $x = 0$ of the depth dose curve is selected as the coordinate of the marker — the point at which the dose value is significantly greater than at neighboring points on the dosimetric film. Figure 3 shows the results of dose measurements for electron beam incidence angles $\theta = 0^\circ$ and 45° on the surface of the dosimetric wedge, which are normalized to the average dose value on the upper surface of the dosimetric wedge (see Fig. 2).

To analyze the measurement results, we highlight three spatial areas, which are separated in the figure by vertical dotted lines.

Area 1 – the dose in the film located on the upper surface of the dosimetric wedge and that in the film when the film enters the dosimetric wedge. The measurement results in this area cannot be used to describe the depth dose curves, since they are distorted by boundary effects in the design of the dosimetric wedge and the positioning of the marker on the film.

Area 2 – the dose in the film located at a sufficient distance from the boundaries of the dosimetric wedge. The measurement results in this area are suitable for describing the depth dose curves.

Area 3 – the dose in the film, where the dose values are determined by the bremsstrahlung from the electron beam passing through the dosimetric wedge to this area, the so-called bremsstrahlung tail. The measurement results in this area cannot be used for comparison with the results of calculations based on semi-empirical models, since the models take into account the dose formation only due to the ionization losses of electrons.

Thus, the data obtained on the basis of measurements of depth dose curves by the dosimetric wedge method can be used to describe depth dose curves only in a limited depth range. To validate the models, it is necessary to extract the ionization component of the dose from this data.

Determination of the basic parameters of the model based on the results of measuring the depth dose curve

Semi-empirical models of the depth dose curve for an electron beam incident on a semi-infinite medium at an angle θ are based on relationships in the form of integral transformations of the depth dose curve for normal incidence of the radiation beam on the medium [27,28]. Therefore, processing the measurement results with the objective to obtain the depth dose curve for normal incidence of the electron beam on a semi-infinite medium is the first step in determining the model parameters. As shown in the previous section, the data that can be obtained based on measurements by the dosimetric wedge method correctly describes the depth dose curve only at a sufficient distance

from the irradiated surface of the dosimetric wedge. In the integral transformations applied in the models, the depth range near the surface of the irradiated object makes a significant contribution to the results. Therefore, special methods of processing the measurement results are required for the correct extrapolation of the depth dose curve in the shallow depth range in the wedge. For this purpose, the processing of the measurement results of the depth dose curve in the film at normal incidence of the electron beam on the wedge was carried out using a two-parameter electron beam model (PFSEM method), i.e., by fitting the parameters of a semi-empirical model [34].

The red solid curve in Fig. 4 presents the result of a two-parameter fit with the following PFSEM method parameters: monoenergetic electron beam energy is $E_0 = 9.84 \text{ MeV}$ and additional layer thickness corresponding to the displacement in the film is $X_0 = 0.87 \text{ cm}$. The dotted curve is calculated in the result of a single-parameter fit with the following PFSEM method parameter value: monochromatic electron beam energy is $E_1 = 8.4 \text{ MeV}$. As one can see in Fig. 4, the two-parameter fitting of PFSEM measurement results provides a more accurate approximation of measurement results and extrapolation of the depth dose curve to the shallow depth region in the wedge than standard one-parameter method.

It should be noted that the obtained approximation of the depth dose curve in the film under normal incidence of the electron beam on the wedge contains the contribution of bremsstrahlung to the dose value. In Fig. 4, the dotted horizontal line shows the level of the bremsstrahlung tail. Since the models take into account the dose formation only due to ionization losses of electrons, it is necessary to exclude the contribution of bremsstrahlung from the approximation of the depth dose curve. To do this, the value of the contribution of bremsstrahlung to the dose is assumed to be independent of the depth. The value of this contribution is calculated as the average dose in the region 3 - the tail of the bremsstrahlung and subtract the obtained value of the contribution from the dose values at all depths. The result of excluding the contribution of bremsstrahlung from the depth dose curve is shown in Fig. 5. The model parameter L_{max} is determined from the curve in Fig. 5. This parameter is the depth to which the values of the depth dose curve in the film are known. The parameter is determined as the maximum value of the depth x to which all dose values $D(x) > 0$. For the data in Fig. 5, the model parameter $L_{max} = 6.6 \text{ cm}$.

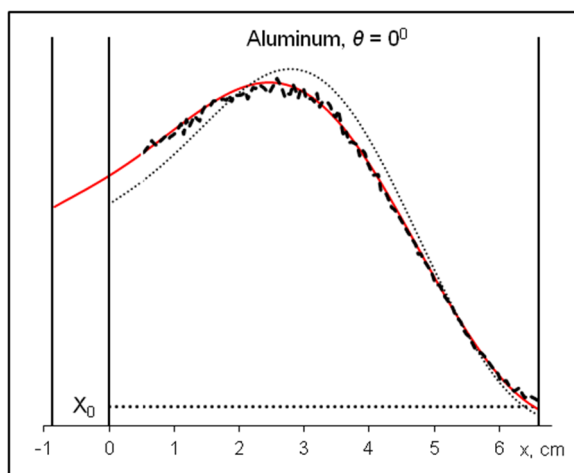


Figure 4. Results of processing the measurements of the depth dose curve in the film (dashed curve) using the PFSEM method. The red solid curve corresponds to the two-parameter fit. The dotted curve corresponds to the single-parameter fit.

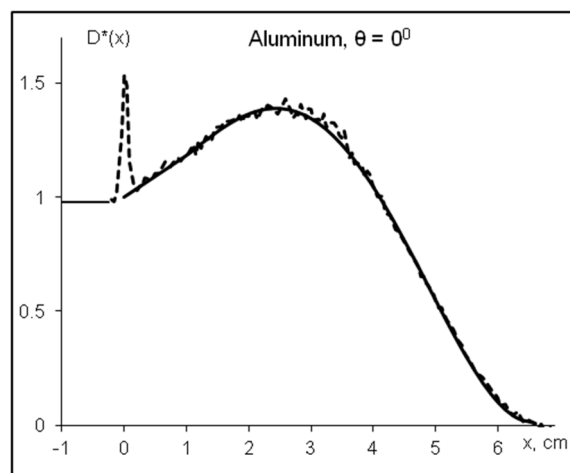


Figure 5. Depth dose curve in the film due to ionization losses of electrons, with normal incidence of the electron beam on the wedge – basic dependence for semi-empirical models.

The solid curve in Fig. 5 shows the depth-dose curves in the film when the electron beam strikes the wedge normally, which is prepared for use in semi-empirical models as basic data for calculations. In the following, the characteristics for these depth-dose curves are calculated in accordance with standards [4, 6]. These parameters are: the practical range of electrons R_p and the depth of half the maximum dose reduction R_{50} . The characteristics of the dose-depth dependence curves (R_p, R_{50}) relate to the parameters of the PFSEM method (E_0, X_0) by the following relationships [8]:

$$R_p = R_p(E_0) - X_0 \cdot K_w; R_{50} = R_{50}(E_0) - X_0 \cdot K_w, \quad (1)$$

where $R_p(E_0)$ is practical range of electrons and $R_{50}(E_0)$ is the depth of half the maximum dose reduction for electrons with energy E_0 , K_w is the ratio of film distance to the depth in dosimetric wedge (for standard aluminum dosimetric wedge, this ratio is $K_w = 0.28$).

Using eq. (1) and the values of the parameters (E_0, X_0) determined during processing the measurement results (see Fig. 4) by the PFSEM method, one obtains $R_p = 1.75 \text{ cm}$, $R_{50} = 1.32 \text{ cm}$. Based on these values (R_p, R_{50}), according to the standard [6], characteristics of the electron energy: average energy E_{Av} and most probable energy E_p of the electron source, are determined: $E_{Av} = 8.47 \text{ MeV}$, $E_p = 8.77 \text{ MeV}$. Note that the energy value $E_1 = 8.4 \text{ MeV}$, calculated based on a single-parameter PFSEM fit, is close to the energy value E_{Av} .

Determination of fitting parameters for semi-empirical models of the depth dose curve

The basic relationship for the depth dose curve in a semi-infinite medium $D(x, \theta, E)$, under uniform irradiation with a monoenergetic electron beam with energy E at an angle θ to the surface of the medium, can be represented as an integral transformation of the depth dose curve in a semi-infinite medium $D(x, 0, E)$, when the medium is irradiated with a normally incident electron beam

$$D_i(x, \theta, E) = \int_0^{L_{max}} D(t, 0, E) \cdot K_i(t, x, \theta, \alpha_i(E), Q_i(E)) dt \tag{2}$$

where $K_i(t, x, \theta, \alpha_i(E), Q_i(E))$ is the kernel of the integral transform; $\alpha_i(E), Q_i(E)$ are fitting parameters of semi-empirical models; for the *Dose-Map* object model with uniform dose distribution, the index $i=1$, and for Gaussian distribution, the index $i=2$.

In semi-empirical models [27], power functions are used to approximate the distribution of transmitted energy in the volume of matter, which is initiated by the normal incidence of a point beam of radiation on the surface of a semi-infinite medium (*Dose-Map* object).

$$F(x, \alpha, Q) = \alpha \cdot L_{max} \left(\frac{x}{L_{max}} \right)^Q, \quad \alpha > 0, \quad Q \geq 0, \quad 0 < x \leq L_{max} \tag{3}$$

Therefore, these models have two fitting parameters: Q - the exponent of the power function and α - a multiplier that determines the maximum value of the function $F_{max} = \alpha \cdot L_{max}$. Due to the axial symmetry of the *Dose-Map* object, the dependence of the radius $R(x) = F(x, \alpha, Q)$ of the circle is used to describe uniform distribution, and the dependence of the dispersion $\sigma(x) = F(x, \alpha, Q)$ on the depth x in the medium is used for Gaussian distribution.

The procedures for determining the fitting parameters of semi-empirical models were described in [28]. However, the calculation results were presented there only for monoenergetic electron beams. Industrial radiation facilities typically have electron beams with a fairly broad spectrum. In this case, the depth dose curve $D(x, \theta)$ can be calculated as the average of the depth dose curves $D(x, E, \theta)$ according to the spectral distribution of electrons $S(E)$:

$$D(x, \theta) = \int_{E_{min}}^{E_{max}} D(x, \theta, E) \cdot S(E) dE \tag{4}$$

Here E_{min} and E_{max} are minimum and maximum electron energy in the beam. Substituting Eq. (2) into Eq. (4) and changing the order of integration, one obtains

$$D_i(x, \theta) = \int_0^{L_{max}} \int_{E_{min}}^{E_{max}} D(t, 0, E) \cdot K_i(t, x, \theta, \alpha_i(E), Q_i(E)) \cdot S(E) dE dt \tag{5}$$

If the spectral distribution $S(E)$ and the fitting parameter functions of the models $\alpha_i(E)$ and $Q_i(E)$ are known for irradiation by the electron beam with the given spectrum, then eq. (5) makes it possible to calculate the depth dose curve $D_i(x, \theta)$. However, detailed information about the spectrum and the dependence of the model fitting parameters on electron energy is usually unavailable.

To develop the approximate calculation method, when integrating the energy in eq. (5), the model fitting parameters are assumed to be constants equal to $\alpha_i(E_{Av})$ and $Q_i(E_{Av})$. In this case, one derives the expression

$$D_i(x, \theta) = \int_0^{L_{max}} D(t, 0) \cdot K_i(t, x, \theta, \alpha_i(E_{Av}), Q_i(E_{Av})) dt \tag{6}$$

Here $D(t, 0)$ is the dose depth curve in semi-infinite medium under irradiation by normally incident electron beam with a given spectrum,

$$D(t, 0) = \int_{E_{min}}^{E_{max}} D(t, 0, E) \cdot S(E) dE \tag{7}$$

It should be noted that the simple method for calculating the depth dose curve in accordance with the following expression was suggested in [27]:

$$D(x, \theta) = \int_0^{L_{max}} D(t, 0, E_{Av}) \cdot K_i(t, x, \theta, \alpha_i(E_{Av}), Q_i(E_{Av})) dt \tag{8}$$

However, the results obtained by this method appeared to be unsatisfactory because of the difference between the depth dose curve $D(t, \theta, E_{Av})$ and the approximation of the dose measurement results $D(t, \theta)$, which is shown in Fig. 4. The

application of the exact dependence of the depth dose curve $D(t, \theta)$ in eq. (6) ensures satisfactory accuracy of the model predictions.

In the proposed method based on eq. (6), to determine the fitting parameters of the semi-empirical model, it is sufficient to determine the values of these parameters for a monoenergetic electron beam with energy E_{Av} . The procedure for determining the fitting parameters of semi-empirical models, as described in [28], is used in the present paper.

The fitting parameters of the semi-empirical model are determined from the condition of equality of the value of the optimal layer thickness H_{opt} during two-side electron irradiation, obtained by modelling the depth dose curves using the Monte Carlo method, to the value of the optimal layer thickness calculated using the semi-empirical model with these parameters. The implemented method is as follows.

1. The irradiation mode is selected: electron energy E and angle θ of incidence of the beam on the surface of the object undergoing the radiation treatment. The selected irradiation mode of the object should ensure a strong dependence of the results of the depth dose curve calculation on the fitting parameters of the semi-empirical model.
2. The depth dose curve for the selected irradiation mode is determined based on modelling the electron passage through the semi-infinite medium by the Monte Carlo method. The depth dose curve calculated using the Monte Carlo method is shown in Fig. 6 in the form of the histogram.
3. The optimal layer thickness H_{opt} is determined for two-side electron irradiation using the depth dose curve calculated by the Monte Carlo method. The optimal layer thickness H_{opt} is determined by searching through layer thickness values with the step of 0.01 g/cm^2 . The search for thicknesses is stopped when the layer thickness is found for which the difference between the dose at the centre and the dose at the surface of the layer has a minimum positive value. The depth dose curve in the layer of optimal thickness under two-side electron irradiation is shown in Fig. 7 by dashed curve.
4. The parameters of the semi-empirical models are determined from the condition of equality of the value of the optimal layer thickness H_{opt} , obtained on the basis of the depth dose curve calculated by the Monte Carlo method, to the value of the layer thickness obtained on the basis of calculations using the semi-empirical model. The parameters of the semi-empirical model are determined by searching through parameter values with the step of 0.01. The depth dose curves calculated with the selected parameters for the semi-empirical model with the uniform distribution (solid curves) and the Gaussian distribution (dotted curves) of the dose in the cross-sections of the *Dose-Map* object are shown in Figs. 6 and 7.

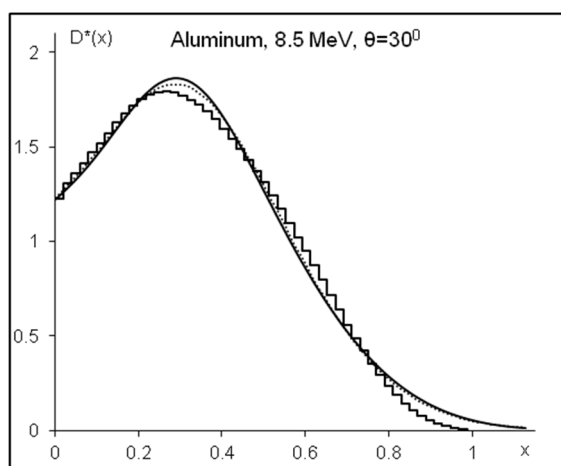


Figure 6. Depth dose curves calculated for a semi-infinite medium. A histogram corresponds to a Monte Carlo simulation.

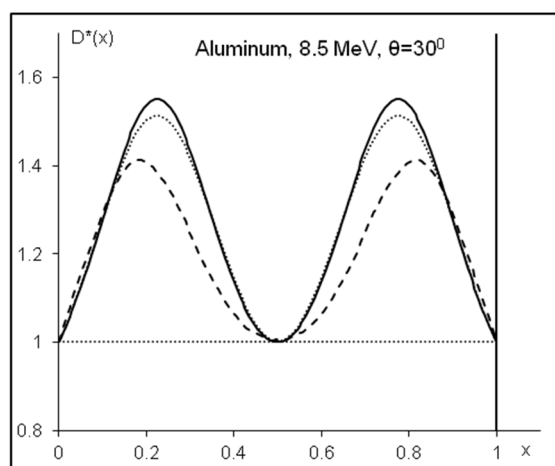


Figure 7. Depth dose curves in a layer of optimal thickness $H_{opt} = 6.7 \text{ g/cm}^2$ with two-sided irradiation. The dashed curve corresponds to the Monte Carlo simulation.

COMPARISON OF MODELLING RESULTS WITH MEASUREMENT RESULTS

The depth dose curves are calculated in semi-empirical models using eq. (4). This equation uses $D(t, \theta)$ - the depth dose curve prepared on the basis of processing the measurement results described in the previous section of the present paper. To determine the fitting parameters of the models, the method proposed in the previous section of the present paper is used. The irradiation mode is selected: the energy of the monoenergetic electron beam is assumed to be equal to the average energy $E_{Av} = 8.5 \text{ MeV}$, calculated based on the processing of the deep dose curve measurement results. The angle θ of the beam incidence on the surface of the dosimetric wedge is assumed to be equal to $\theta = 30^\circ$. The choice of this angle of orientation of the dosimetric wedge ensures sufficiently strong dependence of the results of the depth dose curve calculation on the fitting parameters of the semi-empirical model. However, at this angle of incidence of the electron beam on the layer, the influence of the layer boundary is still insignificant.

The equality of the values of the optimal layer thicknesses, the thickness obtained on the basis of Monte Carlo calculations, and the thickness obtained on the basis of calculations using a semi-empirical model is illustrated in Fig. 7. The depth dose curves shown in Fig. 7 are calculated with the selected parameters $\alpha_1 = 0.8$, and $Q_1 = 1$ for the model with a uniform distribution (solid curves) and with parameters $\alpha_2 = 0.4$, and $Q_2 = 1$ for the model with Gaussian distribution (dotted curves) of the dose in the cross-sections of the *Dose-Map* object. These values of the fitting parameters can be used to calculate depth-dose curves in semi-empirical models for any orientation angle of the dosimetric wedge.

The results of calculations of depth dose curves in semi-empirical models for angles $\theta = 10^\circ, 20^\circ, 30^\circ, 45^\circ$ of the dosimetric wedge orientation are shown in Figs. 8-11.

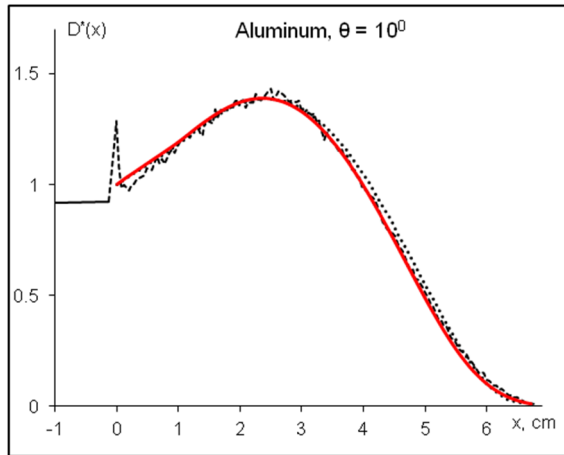


Figure 8. Depth dose curves calculated for a semi-infinite medium. The red curve corresponds to the calculation in the *SEM2U* model. The dotted curve relates to the base curve for the *SEM2U* and *SEM2N* models

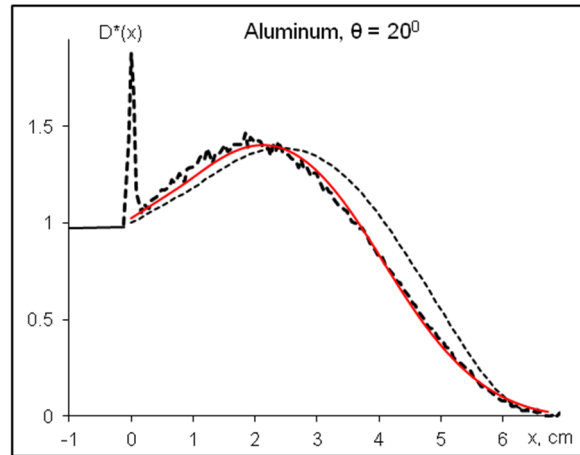


Figure 9. Depth dose curves calculated for a semi-infinite medium. The red curve relates to the calculation in the *SEM2U* model. The dotted curve corresponds to the baseline curve for the *SEM2U* and *SEM2N* models

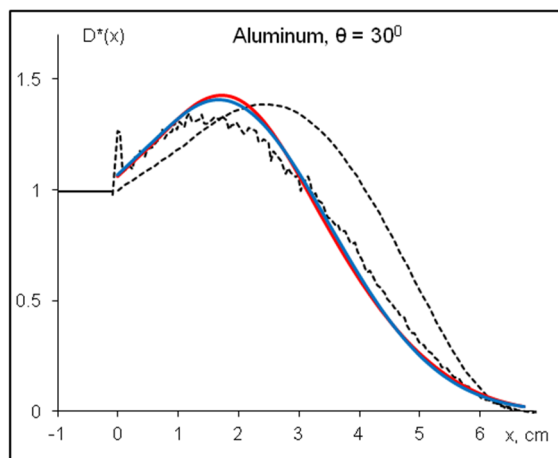


Figure 10. Depth dose curves calculated for a semi-infinite medium. The red curve relates to the calculation in the *SEM2U* model. The blue curve corresponds to the calculation in the *SEM2N* model

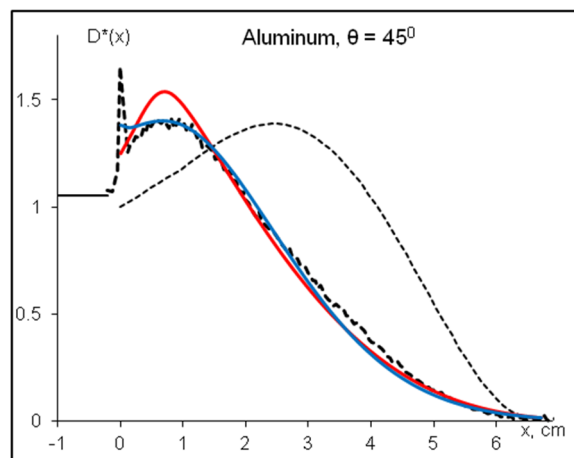


Figure 11. Depth dose curves calculated for a semi-infinite medium. The red curve represents the calculations in the *SEM2U* model. The blue curve relates to the calculations in the *SEM2N* model

The red curves represent calculations in a model with uniform dose distribution, and the blue curves represent calculations in a model with Gaussian dose distribution in the *Dose-Map* object cross-sections. The dashed curves represent depth-dose measurements carried out at different orientations of the dosimetric wedge. The dotted curves represent the depth-dose curve for normal incidence of the electron beam on the dosimetric wedge, which is used as baseline data for calculations in semi-empirical models.

As one can see in Figs. 8 and 9, at small angles of orientation of the irradiation object, the depth dose curve (red curve) does not differ significantly from the depth dose curve (dotted curve) at normal incidence of the electron beam. In this case, there is good agreement between the simulation results and the measurements. It should be noted that the results of calculations using the two models at small angles of orientation of the irradiation object differ only due to rounding errors in the calculations.

As the orientation angle increases, the difference between the results of calculations using the two models increases, as one can clearly see in Figs. 10 and 11. These differences are related to the influence of the boundary on the dose distribution in the cross-sections of the *Dose-Map* object. Therefore, the difference between the calculation results

using the two models can serve as an indicator of the correctness of the basic assumption that the parameters of the *Dose-Map* object in its eigen coordinate system are independent on the angle of incidence of the beam on the layer. As one can see in Fig. 11, the model with a Gaussian distribution (blue curve) of the dose in the cross-sections of the *Dose-Map* object describes the results of measurements of the depth dose curve near the irradiation surface more adequately.

The large error in the model description of the measurement results should be noted in Fig. 10 at the orientation angle of 30° . This is explained by changes in the irradiation mode happened on different days. Such differences indicate instability in the radiation sterilization process during a single batch of the treated product.

CONCLUSIONS

The method of electron beam irradiation with specified beam-incidence angles on the surface of the irradiated object is proposed.

The object is assumed to be placed on a special platform with a variable angle of inclination. The platform is assumed to be installed on the conveyor line of the radiation technology unit.

The method is proposed to measure the depth-dose curve at specified object-orientation angles during electron-beam irradiation. The dosimetric wedge is assumed to be placed on a special platform with a specified angle of inclination, which is installed on the conveyor line of the radiation technology facility. For this method, the dependence of the electron flux $\Phi(\theta)$ incident on the surface of the object on the change in the orientation angle θ of the irradiated object is determined as $\Phi(\theta) = \Phi_0 \cos(\theta)$.

Based on the proposed method, measurements of depth dose curves are carried out in a standard aluminum dosimetric wedge at wedge orientation angles $\theta = 0^\circ, 10^\circ, 20^\circ, 30^\circ, 45^\circ, 60^\circ$.

The results of measurements across three spatial regions at different depths within the wedge are analyzed. It is shown that data obtained from depth-dose curve measurements using the dosimetric wedge method are applicable only within a limited depth range and that specialized methods for processing these data are required when testing semi-empirical models.

Special methods are developed for processing measurement results to correctly approximate and extrapolate the depth dose curve in the shallow depth region of the wedge, based on the *PFSEM* method, i.e. the two-parameter fitting method of the semi-empirical model. A method for excluding the contribution of bremsstrahlung from depth-dose curve measurements is proposed and implemented, as required for comparisons with model-based calculations. The basic depth-dose distribution curve is determined and serves as the basis for calculations in semi-empirical models.

The basic depth dose distribution curve is obtained using special methods developed in the present paper for processing measurements of depth dose distribution curves on a film under normal incidence of an electron beam on a wedge. For this curve, in accordance with the standard [6], the values of electron energy characteristics, such as the average energy E_{Av} and most probable energy E_p of the electron source, are determined. For this depth dose curve, the values of the electron energy characteristics, namely, average energy E_{Av} and most probable energy E_p of the electron source are determined.

A method for determining fitting parameters for semi-empirical models is proposed. It is based on the assumption that these parameters are independent of electron energy. In this method, a base curve derived from processed measurement results is used in the integral transformation. The fitting parameters of semi-empirical models $\alpha_i(E_{Av})$ and $Q_i(E_{Av})$ are determined based on the values of these parameters for the case of a monoenergetic electron beam with energy E_{Av} . The values of the fitting parameters are determined for the model with the uniform distribution ($\alpha_1 = 0.8, Q_1 = 1$) and for the model with the Gaussian distribution ($\alpha_2 = 0.4, Q_2 = 1$) of the dose in the cross-sections of the *Dose-Map* object.

The measurement results are compared with the simulation results from the depth dose curves in semi-empirical models for angles $\theta = 10^\circ, 20^\circ, 30^\circ, 45^\circ$ of the dosimetric wedge orientation. At small angles of orientation of the irradiated object, good agreement between the simulation and measurement results is observed. In these cases, the results of calculations using the two models differ only due to rounding errors.

As the orientation angle increases, the difference between the results of calculations using the two models widens due to the boundary's influence on the dose distribution in the *Dose-Map* object cross-sections. Therefore, the difference between the results of calculations using the two models can serve as an indicator of the model error. It should be noted that the model with a Gaussian dose distribution in the cross-sections of the *Dose-Map* object more adequately describes measurements of the depth dose curve near the irradiation surface.

It is found that changes in the irradiation regime during radiation sterilization can significantly increase the discrepancy between the model description and the measured depth-dose curve.

ORCID

© Valentín T. Lazurik, <https://orcid.org/0000-0002-8319-0764>; © Igor O. Girka, <https://orcid.org/0000-0001-6662-8683>;

© Oleksandr O. Zolotukhin, <https://orcid.org/0000-0003-4440-240X>; © Zbigniew Zimek, <https://orcid.org/0000-0002-8653-5609>

REFERENCES

- [1] S. Schiller, U. Heisig, and S. Panzer, *Electron Beam Technology*, (John Wiley & Sons Inc, 1995).
- [2] M. Reiser, *Theory and Design of Charged Particle Beams*, (John Wiley & Sons, 2008).

- [3] R.C. Davidson, and H. Qin, *Physics of Intense Charged Particle Beams in High Energy Accelerators*, (World Scientific, Singapore, 2001).
- [4] ICRU REPORT 35, *Radiation dosimetry: electron beams with energies between 1 and 50 MeV*, (ICRU, 1984), p. 168.
- [5] R.J. Woods, and A.K. Pikaev, *Applied radiation chemistry: radiation processing*, (Wiley, New York, 1994).
- [6] ISO/ASTM Standard 51649, *Practice for dosimetry in an e-beam facility for radiation processing at energies between 300 keV and 25 MeV*, (ASTM Standards, vol. 12.02, 2005).
- [7] Yu. Pavlov, and P. Bystrov, "Software and hardware complex for radiation processing facility control," *Radiation Physics and Chemistry*, **196**, 110110 (2022). <https://doi.org/10.1016/j.radphyschem.2022.110110>
- [8] V.T. Lazurik, V.M. Lazurik, G.P. Popov, and Z. Zimek, "Dosimetry method based on a two-parametric model of electrons beam for radiation processing," *Problems of Atomic Science and Technology*, **112**(6), 137–141 (2017).
- [9] J.E. Arellano, L.A. Diaz-Torres, J.P. Córdova, J.L. Cervantes, J.A. Elias, M.A. Sosa, and M.A. Vallejo, "Thermoluminescent properties of NASICON glass-ceramics under electron beam irradiation," *Journal of Alloys and Compounds*, **1056**, 186585, (2026). <https://doi.org/10.1016/j.jallcom.2026.186585>
- [10] S. Howard, and V. Starovoitova, "Target optimization for the photonuclear production of radioisotopes," *Applied Radiation and Isotopes*, **96**, 162 (2015). <https://doi.org/10.1016/j.apradiso.2014.12.003>
- [11] R. Pomatsalyuk, S. Romanovskiy, V. Shevchenko, and V. Uvarov, "Real Time Luminescent Dosimetry System for Product Processing at Aa Electron Accelerator," *Problems of Atomic Science and Technology*, (5), 131 (2024). <https://doi.org/10.46813/2024-153-131>
- [12] R.I. Pomatsalyuk, S.K. Romanovsky, V.O. Shevchenko, V.Yu. Titov, D.V. Titov, and V.L. Uvarov, "Analysis of Uncertainty Sources in Dose Measurement at an Industrial Electron Accelerator," *Problems of Atomic Science and Technology*, (5), 117 (2024). <https://doi.org/10.46813/2024-153-117>
- [13] I.V. Melnik, and S.B. Tugay, "Analytical calculations of anode plasma position in high-voltage discharge range in case of auxiliary discharge firing," *Radioelectronics and Communications Systems*, **55**, 514 (2012). <https://doi.org/10.3103/S0735272712110064>
- [14] D. Gregocki, P. Köster, L.U. Labate, S. Piccinini, F. Avella, F. Baffigi, G. Bandini, et al., "Real-Time Dose Monitoring via Non-Destructive Charge Measurement of Laser-Driven Electrons for Medical Applications," *Instruments*, **9**, 25 (2025). <https://doi.org/10.3390/instruments9040025>
- [15] I.A. Ivanov, "Application of the Lambert W Function to the Calculation of the Electron Transmission Coefficient and Bremsstrahlung Yield from the Bethe–Heitler Theory," *Physics of Atomic Nuclei*, (2025). <https://doi.org/10.1134/S1063778825090212>
- [16] I.V. Melnyk, *Radioelectronics and Communications Systems*, **60**, 319, (2017). <https://doi.org/10.3103/S0735272717070056>
- [17] ASTM E2232-21 *Standard Guide for Selection and Use of Mathematical Methods for Calculating Absorbed Dose in Radiation Processing Applications*, (ASTM, 2021), p. 19. <https://doi.org/10.1520/E2232-21>
- [18] F. Salvat, J. Fernandez-Varea, J. Sempau, *PENELOPE 2011: A Code System for Monte Carlo Simulation of Electron and Photon Transport*, (Nuclear Energy Agency, 2012), p. 385.
- [19] S.-T. Jung, S.-H. Pyo, W.-G. Kang, Y.-R. Kim, J.-K. Kim, C.M. Kang, Y.-C. Nho, and J.-S. Park, *Radiation Physics and Chemistry*, **186**, 109506 (2021). <https://doi.org/10.1016/j.radphyschem.2021.109506>
- [20] M. Rezzoug, M. Zerfaoui, Y. Oulhouq, A. Rrhuioua, S. Didi, and D. Bakari, *Radiation Physics and Chemistry*, **235**, 112828 (2025). <https://doi.org/10.1016/j.radphyschem.2025.112828>
- [21] D.J.S. Findlay, *Nucl. Instrum. Methods A*, **276**(3), 598 (1989). [https://doi.org/10.1016/0168-9002\(89\)90591-3](https://doi.org/10.1016/0168-9002(89)90591-3)
- [22] V.L. Uvarov, A.A. Zakharchenko, N.P. Dikiy, Yu.V. Lyashko, R.I. Pomatsalyuk, V.A. Shevchenko, and Eu.B. Malets, *Problems of Atomic Science and Technology*, (6), 180 (2023). <https://doi.org/10.46813/2023-148-180>
- [23] V.L. Uvarov, A.A. Zakharchenko, N.P. Dikiy, R.I. Pomatsalyuk, and Yu.V. Lyashko, *Applied Radiation and Isotopes*, **199**, 110890 (2023). <https://doi.org/10.1016/j.apradiso.2023.110890>
- [24] V.L. Uvarov, A.A. Zakharchenko, N.P. Dikiy, Yu.V. Lyashko, and R.I. Pomatsalyuk, *Radiation Physics and Chemistry*, **214**, 111547 (2024). <https://doi.org/10.1016/j.apradiso.2024.111547>
- [25] M. Rosenstein, H. Eisen, and J. Silverman, *Journal of Applied Physics*, **43**, 3191 (1972). <https://doi.org/10.1063/1.1661684>
- [26] V.G. Rudychev, V.T. Lazurik, and Y.V. Rudychev, *Radiation Physics and Chemistry*, **186**, 109527 (2021). <https://doi.org/10.1016/j.radphyschem.2021.109527>
- [27] I.O. Girka, V.T. Lazurik, Semi-empirical models of electron beam control for radiation sterilisation, *East Eur. J. Phys.* **3**, 422 (2025), <https://doi.org/10.26565/2312-4334-2025-3-45>
- [28] V. Lazurik, S. Sawan, V. Lazurik, and O. Zolotukhin, in: *4th International Maghreb Meeting of the Conference on Sciences and Techniques of Automatic Control and Computer Engineering Proceedings*, (IEEE, Maghreb, 2024), pp. 649–653. <https://doi.org/10.1109/MI-STA61267.2024.10599694>
- [29] I.V. Melnyk, "Simulation of energetic efficiency of triode high voltage glow discharge electron sources with account of temperature of electrons and its mobility in anode plasma," *Radioelectronics and Communications Systems*, **56**, 592 (2013), <https://doi.org/10.3103/S0735272713120066>
- [30] I. Melnyk, A. Pochynok, and M. Skrypka, "Comparison of methods for interpolation and extrapolation of boundary trajectories of short-focus electron beams using root-polynomial functions," *System Research and Information Technologies*, **3**, 77 (2024). <https://doi.org/10.20535/SRIT.2308-8893.2024.3.05>
- [31] S.V. Denbnovetsky, V. I. Melnik, I.V. Melnik, B.A. Tugay, in: *XVIII-th International Symposium on Discharges and Electrical Insulation in Vacuum, Proceedings*, (ISDEIV, 1998), vol. 2, pp. 637–640. <https://doi.org/10.1109/DEIV.1998.738530>
- [32] I. Melnyk, A. Pochynok, M. Skrypka, and O. Demyanchenko, "Method of interpolation using root-fractional-rational functions of different orders," *Bulletin of Taras Shevchenko National University of Kyiv. Physics and Mathematics*, **80**(1), 130-138. (2025). <https://doi.org/10.17721/1812-5409.2025/1.17>

- [33] V. Lazurik, and V. Moskvina, "Monte Carlo calculation of charge-deposition depth profile in slabs irradiated by electrons," Nucl. Instrum. Methods B, **108**(3), 276 (1996). [https://doi.org/10.1016/0168-583X\(95\)01052-1](https://doi.org/10.1016/0168-583X(95)01052-1)
- [34] T. Tabata, P. Andreo, and K. Shinoda, "An algorithm for depth-dose curves of electrons fitted to Monte Carlo data," Radiation Physics and Chemistry, **53**, 205 (1998). [https://doi.org/10.1016/S0969-806X\(98\)00102-9](https://doi.org/10.1016/S0969-806X(98)00102-9)

ЗАСТОСУВАННЯ НАПІВЕМПІРИЧНИХ МОДЕЛЕЙ УПРАВЛІННЯ ПУЧКОМ ЕЛЕКТРОНІВ У ТЕХНОЛОГІЇ РАДІАЦІЙНОЇ СТЕРИЛІЗАЦІЇ

Валентин Т. Лазурик¹, Ігор О. Гірка¹, Олександр О. Золотухін¹, Збігнев Зібек²

¹Харківський національний університет імені В.Н. Каразіна, Харків, Україна

²Інститут ядерної хімії та технологій, Варшава, Польща

Для використання напівемпіричних моделей необхідно аналізувати дані, які регулярно реєструються під час контролю процесів опромінення, та обробляти ці дані для визначення значень параметрів напівемпіричних моделей. У цій роботі як реєстровані дані використано глибинні криві дози, виміряні у Центрі радіаційної стерилізації ІНСТ, Варшава, Польща. Описано метод проведених вимірювань і представлено аналіз особливостей глибинних кривих дози, які було виміряно методом дозиметричного клина. Визначено області глибин, в яких результати вимірювань можуть бути використані без спеціальної обробки в якості значень глибинної кривої дози в дозиметричному клині. Розроблено спеціальні процедури апроксимації та екстраполяції результатів вимірювань для отримання значень базової залежності напівемпіричних моделей - значення глибинної кривої дози при нормальному падінні пучка електронів на напівнескінченне середовище. Розроблено спеціальні процедури обробки результатів вимірювань на базі методу PFSEM (двопараметрична підгонка параметрів напівемпіричної моделі глибинних кривих дози). Запропоновано та реалізовано процедуру виключення внеску гальмівного випромінювання зі значень глибинних кривих дози. Величину цього внеску оцінено як середнє значення дози в інтервалі хвоста гальмівного випромінювання, і припущено, що величина внеску гальмівного випромінювання в дозу не змінюється з глибиною. Запропоновано метод вибору значень параметрів підгонки моделей на основі припущення про слабку залежність параметрів підгонки від енергії електронів. На основі запропонованого методу визначено параметри підгонки напівемпіричних моделей за результатами моделювання методом Монте-Карло глибинних кривих дози при опроміненні шару моноенергетичним пучком електронів. Проведено порівняння результатів вимірювань із результатами розрахунку глибинних кривих дози, виконаних за напівемпіричними моделями, при опроміненні шару пучками електронів з різними кутами падіння на алюмінієвий дозиметричний клин. На основі результатів порівняння обговорено похибки прогнозів моделей і можливість реалізації методів оптимізації процесів опромінення на основі вибору кута падіння електронів на поверхню опромінюваного об'єкта.

Ключові слова: електронно-променева дозиметрія; крива глибини-дози; процеси стерилізації; контроль оптимальних режимів; напівемпірична модель; метод Монте-Карло